

Supplemental information

**FANCD2-dependent mitotic DNA synthesis
relies on PCNA K164 ubiquitination**

Wendy Leung, Ryan M. Baxley, Emma Traband, Ya-Chu Chang, Colette B. Rogers, Liangjun Wang, Wesley Durrett, Kendall S. Bromley, Lidia Fiedorowicz, Tanay Thakar, Anika Tella, Alexandra Sobeck, Eric A. Hendrickson, George-Lucian Moldovan, Naoko Shima, and Anja-Katrin Bielinsky

Figure S1. Generation of PCNAK164R mutant cell lines, related to Figure 1.

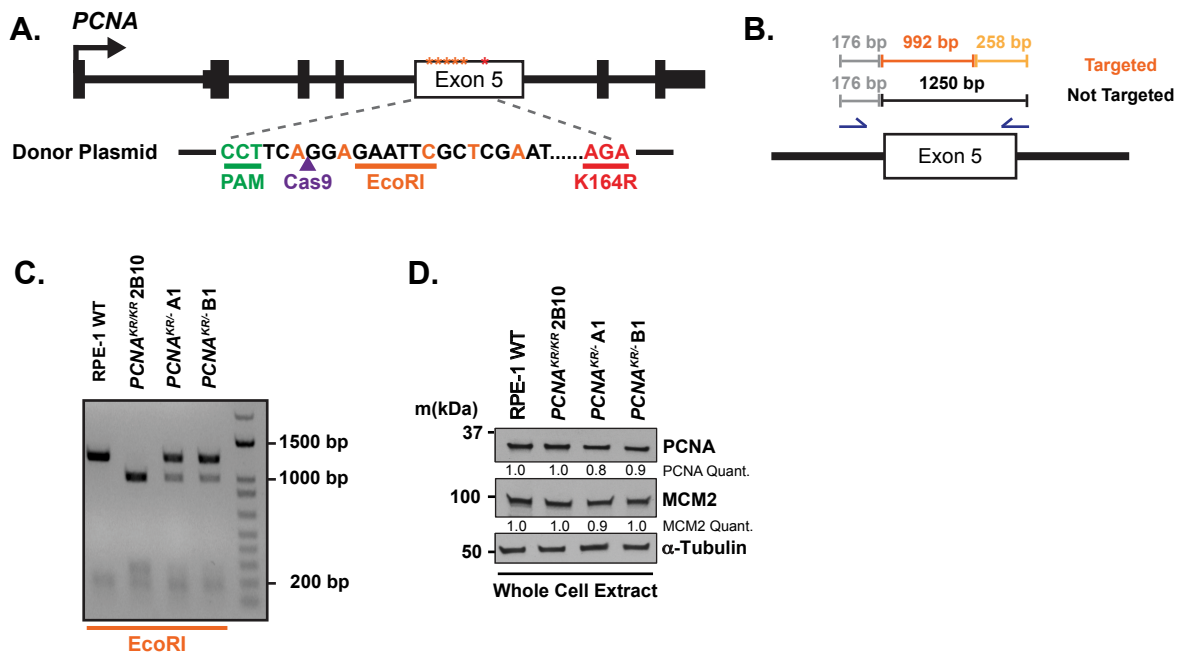


Figure S2. Analysis of the cell cycle, DNA replication and apoptosis in RPE-1 cell lines, related to Figure 2.

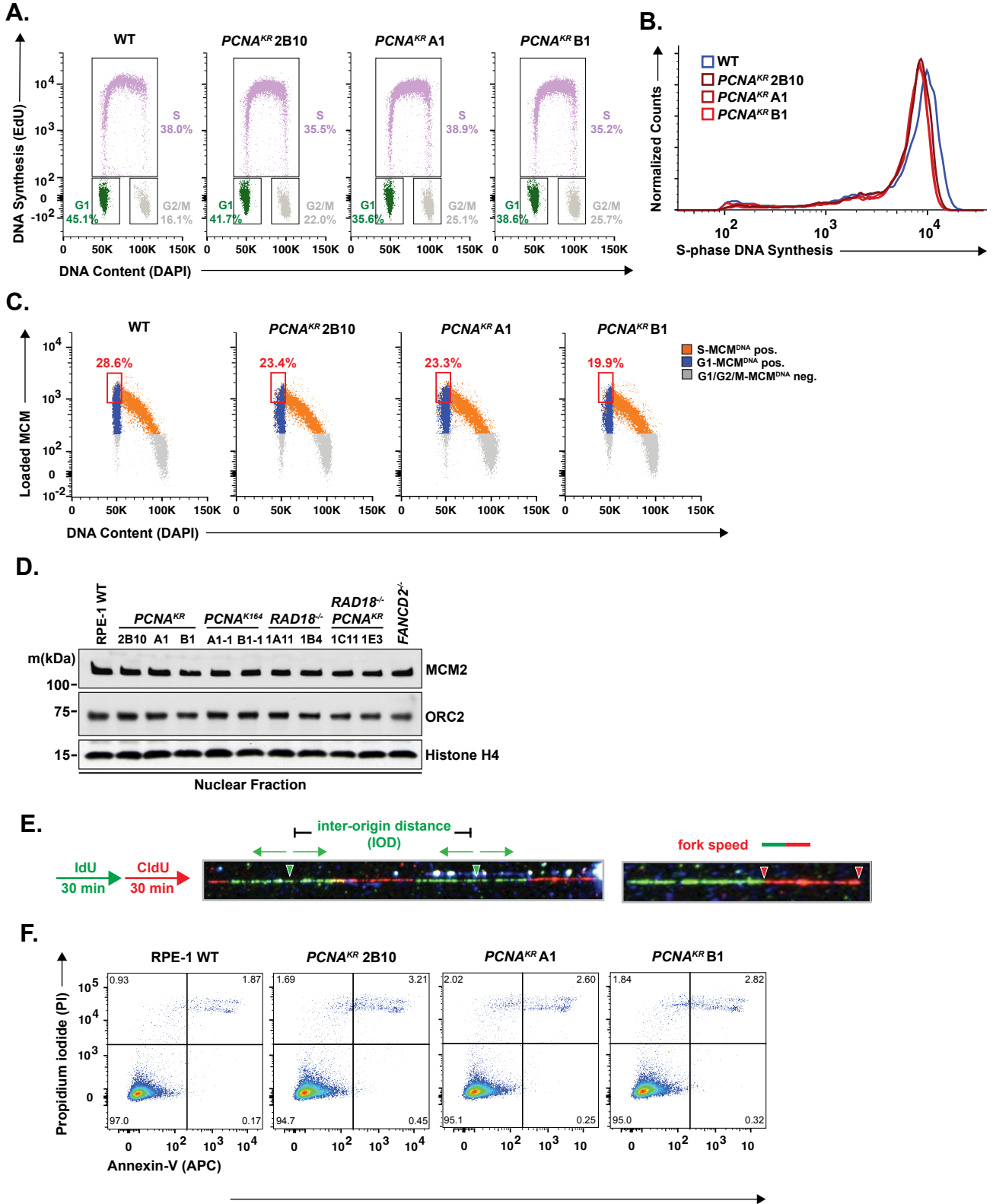


Figure S3. Cell cycle and DNA replication defects in 293T PCNA^{KR} cells, related to Figure 3.

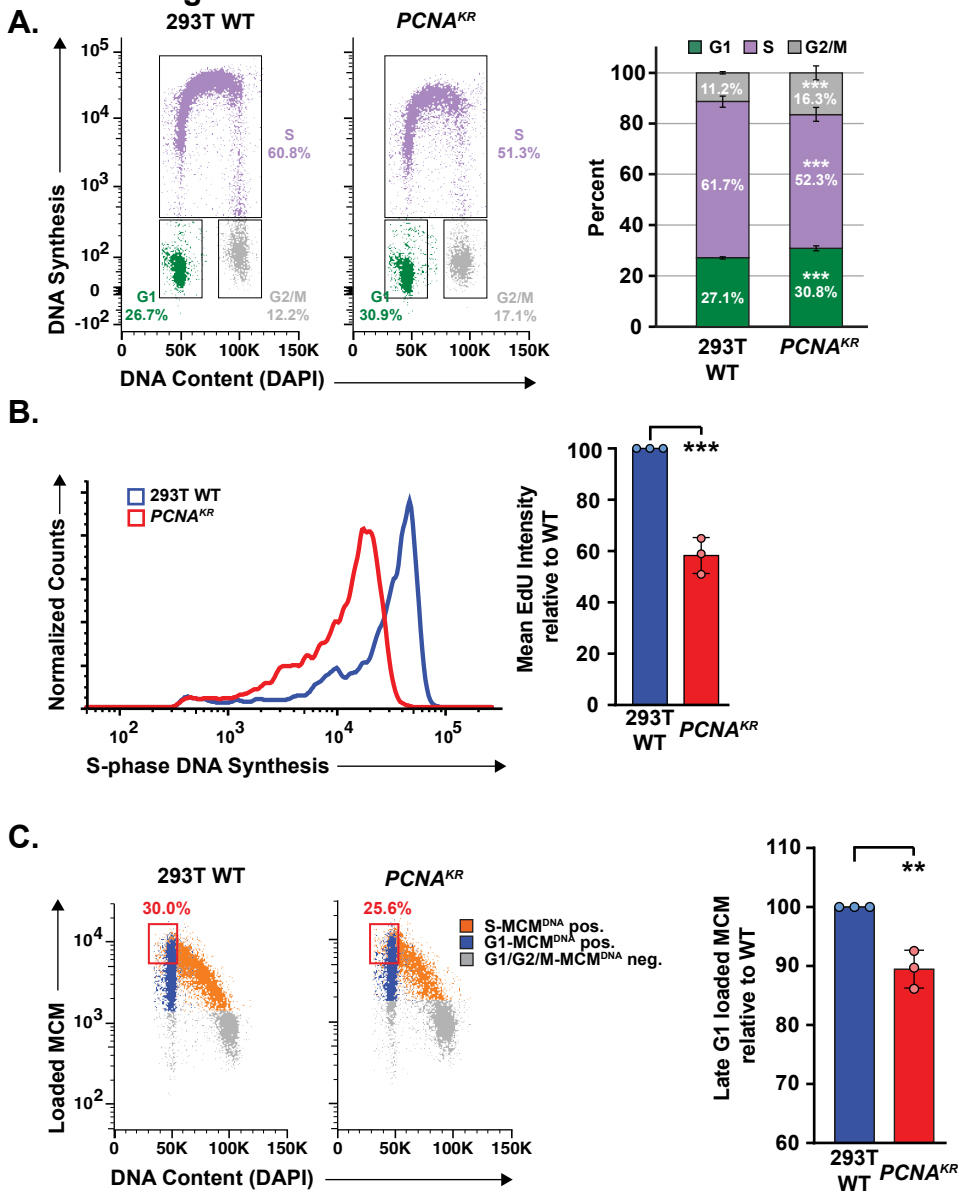


Figure S4. 293T PCNAK164R mutants display increased 53BP1 NBs, related to Figure 3.

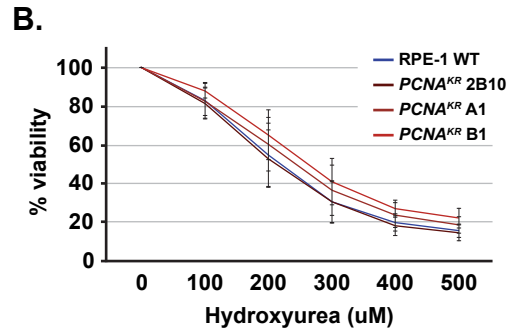
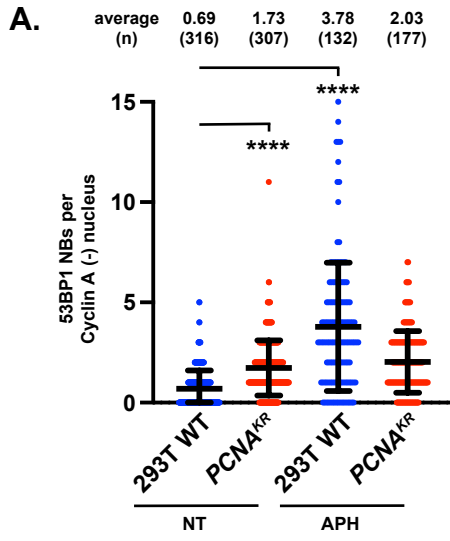
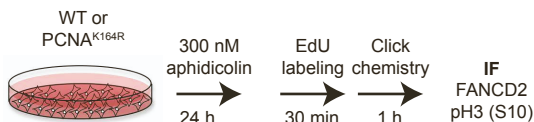
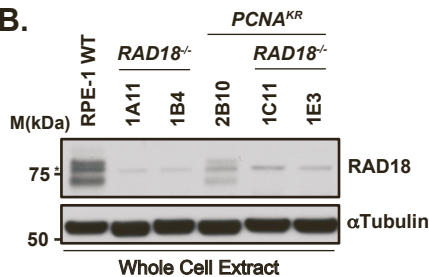


Figure S5. Generation and characterization of mutant RPE-1 cell lines, related to Figure 4.

A.

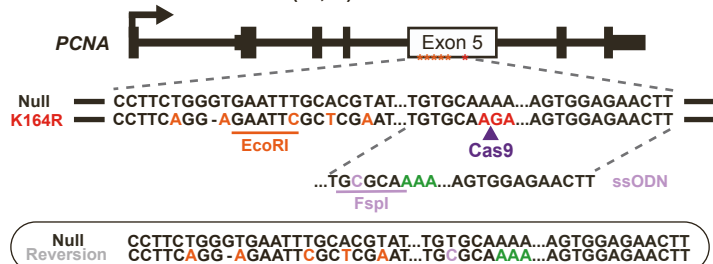


B.



C.

Reversion of PCNA^{KR/-}: A1 (+1, G)



Reversion of PCNA^{KR/-}: B1 (-1, G)

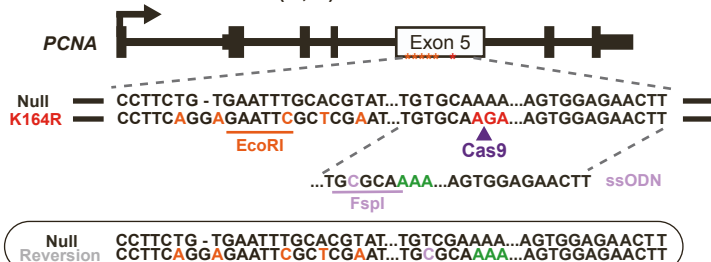
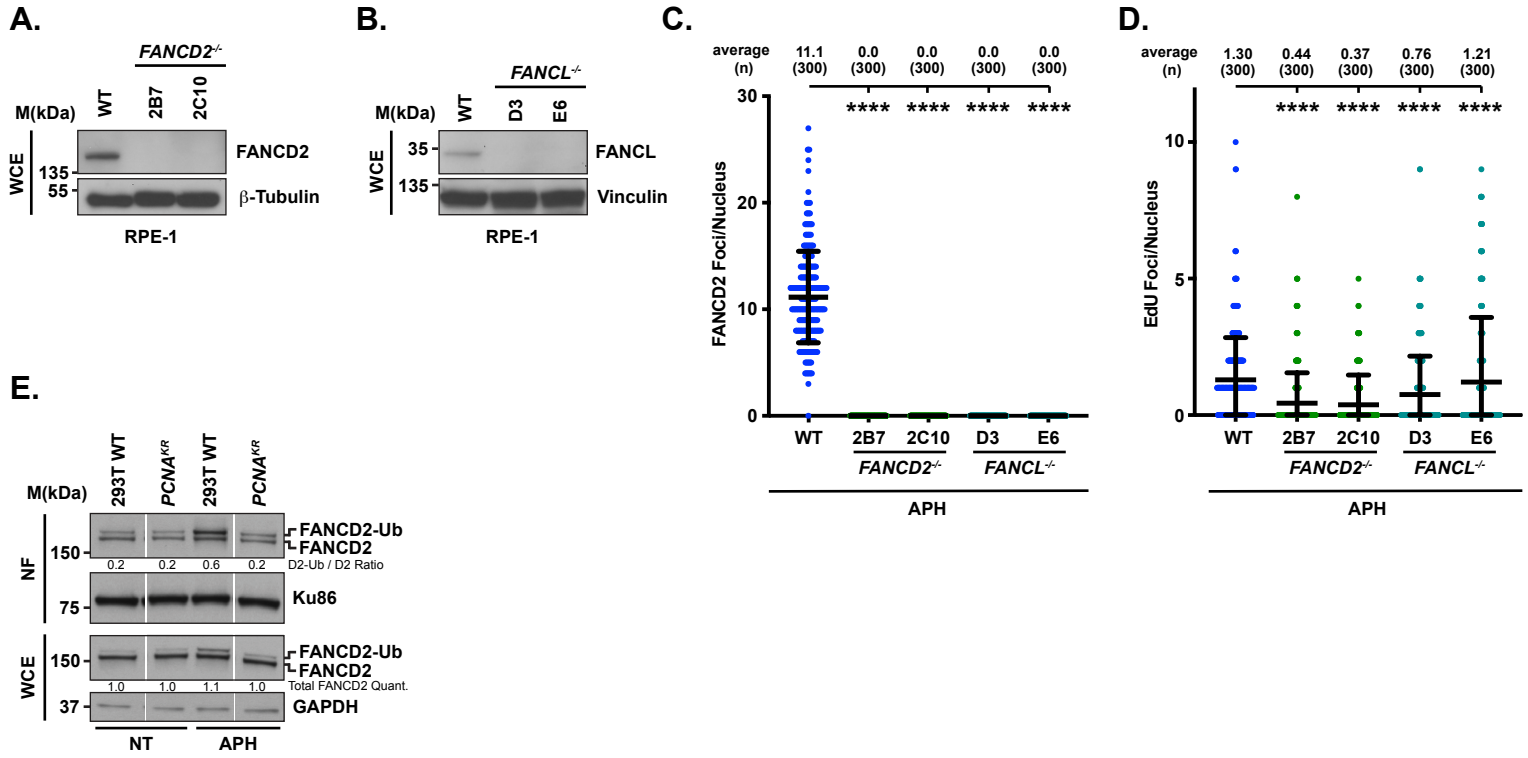


Figure S6. Characterization of the requirement for FANCD2, FANCL and PCNA K164 in RPE-1 and 293T cell lines, related to Figure 5.



SUPPLEMENTARY FIGURE TITLES AND LEGENDS

Supplementary Figure 1. Generation of *PCNA*^{K164R} mutant cell lines

- A)** Schematic of the human *PCNA* indicating that exon 5 was targeted by CRISPR-Cas9. The K164R mutation was knocked-in utilizing a donor plasmid.
- B)** Schematic of screening PCR and expected PCR product sizes after EcoRI restriction enzyme digestion.
- C)** Representative genotyping PCR. Not targeted (wildtype; 176bp, 1250 bp), monoallelic knock-in (KIN) (*PCNA*^{KR/-} A1 and B1; 176 bp, 258 bp, 992 bp, 1250 bp), and biallelic KIN (*PCNA*^{KR/KR} 2B10; 176 bp, 258 bp, 992 bp).
- D)** Western blot analyses of whole cell extracts from wildtype RPE-1 and *PCNA*^{K164R} cells for MCM2 and PCNA with α -tubulin as the loading control. Quantified intensities of MCM2 and PCNA levels were normalized to the loading control.

Supplementary Figure 2. Analysis of the cell cycle, DNA replication and apoptosis in RPE-1 cell lines.

- A)** Representative cell cycle distribution of RPE-1 wildtype and *PCNA*^{K164R} cell lines based on DNA content (DAPI) and DNA synthesis (EdU incorporation). Percentage of each population in G1- (green), S- (purple) or G2/M-phase (gray) is shown.
- B)** Histogram of EdU staining of S-phase cells from RPE-1 wildtype (blue) and *PCNA*^{K164R} cells (maroon/red).
- C)** Representative chromatin flow cytometry plots for RPE-1 wildtype and *PCNA*^{K164R} cells. G1-phase/MCM positive cells (blue), S-phase/MCM positive cells (orange) and G1- or G2/M-phase/MCM negative cells (gray) are indicated. Percentage of MCM2 stained cells in late G1 is indicated (red box).

D) Western blot analyses of nuclear fractions from wildtype RPE-1, *PCNA*^{K164R}, *PCNA*^{K164} reverted, *RAD18*^{-/-}, *RAD18*^{-/-}: *PCNA*^{K164R} double mutant and *FANCD2*^{-/-} cell lines for MCM2 and ORC2 with Histone H4 as a loading control.

E) Example fibers used for DNA combing analyses. Active replication forks were sequentially labeled with IdU (25 μM, green) for 30 minutes followed by labeling with CldU (200 μM, red) for 30 minutes. Inter-origin distance (IOD) is measured as center-to-center distance between two adjacent progressing bidirectional forks. Fork speed is measured as the length of the second (red) label divided by the duration of the labeling period.

F) Representative flow cytometry plots sorting cells based on propidium iodide and annexin V staining for the quantification of live, apoptotic and dead cells in RPE-1 wildtype and *PCNA*^{K164R} cell lines.

Supplementary Figure 3. Cell cycle and DNA replication defects in 293T *PCNA*^{K164R} cells.

A) (Left) Representative cell cycle distribution of 293T wildtype and *PCNA*^{K164R} lines based on DNA content (DAPI) and DNA synthesis (EdU incorporation). Percentage of each population in G1- (green), S- (purple) or G2/M-phase (gray) is shown. (Right) Cell cycle distribution of 293T wildtype and *PCNA*^{K164R} cell lines from three biological replicates. Percentage of each population in G1- (green), S- (purple) or G2/M-phase (gray) is shown. Error bars indicate standard deviation and significance was calculated using students *t-test* with *** > 0.001.

B) Histogram (left) and quantification of mean fluorescent intensity (right) of EdU staining of S-phase cells from 293T wildtype (blue) and *PCNA*^{K164R} cell lines, n = 9 across three biological replicates. Error bars indicate standard deviation and significance was calculated using students *t-test* with * > 0.05.

C) (Left) Representative chromatin flow cytometry plots for 293T wildtype and *PCNA*^{K164R} cells. G1 phase/MCM positive cells (blue), S phase/MCM positive cells (orange) and G1- or G2/M-phase/MCM negative cells (gray) are indicated. Percentage of MCM2 stained cells in late G1 is

indicated (red box). (Right) Quantification of the percentage of MCM2 stained cells in late G1 from 293T wildtype (blue) and *PCNA*^{K164R} (red); n = 9 across three biological replicates. Error bars indicate standard deviation and significance was calculated using students *t*-test with * > 0.05.

Supplementary Figure 4. 293T *PCNA*^{K164R} mutants display increased 53BP1 NBs.

A) 53BP1 NB quantification of untreated and APH treated (450 nM) 293T wildtype (blue) and *PCNA*^{K164R} cells (red). Number (n) of nuclei quantified is listed. Error bars indicate standard deviation and significance was calculated using one-way ANOVA with Tukey's multiple comparison test with *** < 0.001.

B) Comparison of HU sensitivity comparing average percent viability in RPE-1 wildtype and *PCNA*^{K164R} cell lines. Concentrations tested are indicated. Error bars indicate standard deviation and statistical significance was calculated using students *t*-test with * < 0.05; ** < 0.01, *** < 0.001; n = 9-12 replicate wells across three biological replicates for all data points.

Supplementary Figure 5. Generation and characterization of mutant RPE-1 cell lines.

A) Schematic representation of experimental setup of the mitotic DNA synthesis assay.

B) Western blot analyses of whole cell extracts from wildtype, *RAD18*^{-/-}, *PCNA*^{K164R} and *RAD18*^{-/-};*PCNA*^{K164R} RPE-1 cells for RAD18 with tubulin as the loading control.

C) Strategy to revert the mutations in *PCNA*^{K164R/-} clones A1 and B1 to restore expression of wildtype PCNA.

Supplementary Figure 6. Characterization of the requirement for FANCD2, FANCL and PCNA K164 in RPE-1 and 293T cell lines.

A) Western blot analyses of FANCD2 with Tubulin as the loading control in whole cell extracts from wildtype and *FANCD2*^{-/-} RPE-1 cells.

B) Western blot analyses of FANCL with Vinculin as the loading control in whole cell extracts from wildtype and *FANCL*^{-/-} RPE-1 cells.

C) FANCD2 foci quantification from three biological replicates in RPE-1 wildtype (blue), *FANCD2*^{-/-} (green) and *FANCL*^{-/-} (teal) cells treated with 300 nM APH. Number (n) of nuclei quantified is listed. Significance was calculated by Kruskal-Wallis with Dunn's multiple comparison test with *** > 0.001.

D) EdU foci quantification from three biological replicates in RPE-1 wildtype (blue), *FANCD2*^{-/-} (green) and *FANCL*^{-/-} (teal) cells treated with 300 nM APH. Number (n) of nuclei quantified is listed. Significance was calculated by Kruskal-Wallis with Dunn's multiple comparison test with *** > 0.001.

E) Western blot analyses of FANCD2 with Ku86 or GAPDH as the loading control in nuclear fractions (top) or whole cell extracts (bottom) from 293T wildtype and *PCNA*^{K164R} cells with or without 450 nM APH treatment. Quantified band intensities were normalized to loading controls.